Proceedings of the ASNT, NDT of Composites
2015, Seattle WA, 4-6 May 2015

# Free Space Microwave Non Destructive Characterization of Composite Materials

**Jan Obrzut, Ahmed Hassan and Edward Garboczi[1]**
Material Measurement Laboratory, NIST
100 Bureau Dr, Gaithersburg, MD 20899, [1]325 Broadway, Boulder, CO 80305

## INTRODUCTION

We present a free-space microwave experimental measurement system for the non-destructive testing of composite materials that can be either dielectric or electrically conducting and either thinner or thicker than the microwave penetration depth. The system operates in the Q- frequency band of 30 GHz to 50 GHz with a fixed wave propagation distance between free-space antennas. In order to illustrate the efficacy of our technique, we present the analysis of dielectric laminates, as well as of nano-carbon epoxy composites with inter-laminar multi-walled carbon-nanotube structures. These laminates can be microwave absorbing or reflecting, with inter-laminar carbon nanotube networks for enhanced strength-to-weight performance and electrical conductivity. Carbon nanotubes (CNTs) composites have been incorporated in a wide range of applications, especially in the aerospace and automotive industries [1, 2]. The mechanical, thermal and electrical properties of these composites are predominantly determined by the properties and the dispersion of the CNTs in the embedding matrix. During manufacturing, the CNT network evolves from a non-conducting dielectric state through the conductivity percolation transition until the desired properties are obtained [3]. Such changes in properties can be accurately captured by measuring the magnitude and phase of the transmitted and reflected scattering parameters, providing that the measurements are correctly calibrated. Calibration corrects errors from the impedance mismatch between the antennas and free space, and eliminates effects of multiple reflections between the antennas and the material being tested (MUT). One of the error correction method used most often is the Thru- Reflect-Line (TRL) calibration [4- 6], which requires changing the distance between the antennas during the measurements, while assuming that the phase alignment and coupling from the previous steps remains unchanged. The Line-Network-Network (LNN) procedure is another calibration technique. This calibration method does not employ a reflection standard [5]. Instead, it calibrates measurements by using one Thru measurement without the MUT and three additional measurements with the MUT at three locations separated by an equal distance $\Delta x$ [5]. Both, re-positioning of the antennas in TRL or multiple shifting of the MUT in LNN are difficult to implement in quality control and high-thru-put unrolling. In contrast, we have developed a simpler yet accurate error correction model, which requires only two reference measurements of complex scattering parameters. One reference is from a known conductor, such as an aluminum plate, and the other from a wave propagating in an air slab with a geometrical propagation length equal to that of the specimen under analysis.

## EXPERIMENTAL METHODS

The presented non-contact microwave measurement system utilizes conical WR-22 horn antennas connected to a 2 Port vector network analyzer, which simultaneously measures the transmitted and reflected waves in the Q-frequency band, centered at 40 GHz. ($\lambda_0$ = 7.5 mm). The distance between the antennas is fixed at 30 $\lambda o$ and the beam waist diameter of 7 $\lambda o$ is uniform over several $\lambda_0$ along the propagation direction ensuring near plane wave incidence. The measurement of the transmitted scattering parameters, $S_{21}$ and $S_{12}$, is referenced to propagation in known loss-less dielectric (air), while the measurement of the reflected scattering parameters $\mathbf{S}_{11}$ and $\mathbf{S}_{22}$, is referenced to reflection from a metal plate conductor with conductivity much larger than that of the MUT. The sample holder is made of a microwave-transparent net and mounted on a motorized stage for precise positioning of the specimen between the antennas (Figure 1).
The purpose of the precise positioning of the specimens is to create a library of calibration data that could be used in

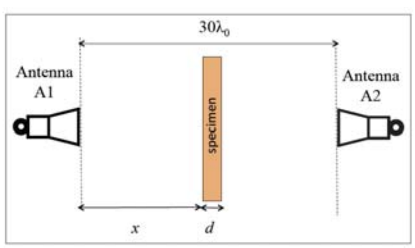


**Figure 1: Experimental set-up**

a variety of testing conditions, in real time, without the need for re-calibration. The measurement technique is capable of providing both the real and imaginary parts of the complex dielectric permittivity or/and conductivity constant. These can be related to the quality of the material and its detailed physical properties, such as dispersion and content of the conducting nano-carbon filler. The technique is quite simple and, therefore, attractive for non-destructive quality control in the manufacturing environment. Specimens considered in this work have lateral dimensions of 300 mm x 300 mm or larger, which minimizes the effects of surface waves propagation and parasitic edge effects.

## Error Correction Model for on-line Non Destructive Testing

The error correction procedure for non destructive testing employs two reference measurements of complex scattering parameters. One reference is a reflection from a known conductor, such as an aluminum plate, and the other from a wave propagating in an air slab with a geometrical propagation length equal to that of the specimen being tested. The uncorrected complex scattering parameters of the MUT denoted $\{\boldsymbol{T}_{11}, \boldsymbol{T}_{21}, \boldsymbol{T}_{22}, \boldsymbol{T}_{21}\}$ are measured in the frequency range of 30 GHz to 50 GHz. The measurement system is initially calibrated at the coaxial ends connected to the antennas (see Fig. 1). However, the free space measurements are still affected by propagation through antennas A1 and A2, and by air propagation between antennas and the specimen surfaces. In order to account for these effects and to move the reference planes of the measurements from the coaxial ends to the plane of the MUT, two additional reference measurements are performed using standards with known propagation characteristics. As already indicated, these standards are (*i*) metal plate, for which we denote the scattering parameters as $\{\boldsymbol{M}_{11}, \boldsymbol{M}_{22}\}$ and (*ii*) the scattering parameters from *air*, without MUT , denoted $\{\boldsymbol{L}_{11}, \boldsymbol{L}_{21}, \boldsymbol{L}_{22}, \boldsymbol{L}_{21}\}$. The corrected reflection $\boldsymbol{S}_{11\text{-cr}}$, and transmission, $\boldsymbol{S}_{21\text{-cr}}$, scattering parameters from the MUT [7] are given by expressions (1) and (2):

$$\boldsymbol{S}_{11-\mathrm{cr}} = \frac{G[\boldsymbol{T}_{11} - \boldsymbol{L}_{11}]}{G[\boldsymbol{M}_{11} - \boldsymbol{L}_{11}]}(-1) \quad (1), \text{ and } \quad \boldsymbol{S}_{21-\mathrm{cr}} = \frac{G[\boldsymbol{T}_{21}]}{\mathrm{G}[\boldsymbol{L}_{21}]}\exp(-j\beta_0 d) \quad (2)$$

where, $d$ is the MUT thickness, $\beta_0 = \omega/c_0$ is the plane wave propagation factor in air, the scattering parameters, $\boldsymbol{T}_{ij}$, $\boldsymbol{M}_{ij}$, and $\boldsymbol{L}_{ij}$ (i,j=1,2) are defined as before, and the procedure $G$ refers to time gating or band filtering of spurious reflections. The gating procedure can be performed by transforming the measurements to the time domain using the Inverse Fast Fourier Transform (IFFT). The reflection/transmission from MUT can then be isolated by multiplying the time domain measurement with a Gaussian window centered at the same time instant as the maximum of the first reflection/transmission. The width of the Gaussian window is selected to capture the response from the MUT. Alternatively, one may use band-pass filtering, which is somewhat less accurate than time gating, but much simpler to implement for on-line automated data processing. In (2), the division by $G[\boldsymbol{L}_{21}]$ normalizes and de-convolutes the antenna response. The multiplication by factor $\exp(-j\beta_0 d)$ brings the reference plane to the MUT surface. In equation (1), subtraction of $\boldsymbol{L}_{11}$ removes the impedance mismatch between the antennas whereas division by $G[\boldsymbol{M}_{11}\text{-} \boldsymbol{L}_{11}]$ normalizes the reflection of the MUT, to that of the metal reference. Since the plate is made of a metallic conductor and will effectively reflect all the incident microwaves, we can assume no transmission from the metal reference, $\boldsymbol{M}_{21} = \boldsymbol{M}_{12} = 0$. The multiplication by -1 in equation (2) is performed to account for the fact that the reflection from the metal plate is 180º out of phase from the incident wave. Following the correction procedure, the corrected $\boldsymbol{S}_{11\text{-cr}}$ and $\boldsymbol{S}_{21\text{-cr}}$ from (1) and (2) can be used directly as quality indicators or they can be de-convoluted to extract the materials characteristic properties, such as the transmission and absorption coefficients, shielding effectiveness or to compute the complex dielectric permittivity or conductivity through a root searching algorithm [7, 8].

## RESULTS and DISCUSSION

Having determined the reference scattering parameters $\boldsymbol{M}_{ij}$ and $\boldsymbol{L}_{ij}$, the scattering parameters of the MUT are measured and corrected. It takes typically a fraction of second to run the entire Q–band frequency scan, collect the data and correct them through equations (1) and (2). Figure 2 illustrates the corrected scattering parameters measured for two epoxy laminate composite materials, C1 and C2, modified with multi-walled carbon nanotubes. The two composite materials contain a similar amount, about 9 % by mass, of highly conducting multi-walled carbon nanotube (MWCNT) network, but they differ in their laminar construction [3]. Composite C1 is reinforced with glass-fabric modified with MWCNTs, and is nominally 1 mm thick. Composite C2 contains additional reinforcement of T300 carbon fabric and its nominal thickness is 2 mm. According to Figure 2, these differences in construction have a profound effect on the microwave response. We applied band pass filtering in the frequency domain to minimize spurious reflections in the corrected data. Gating in the time domain, is more accurate, but it is more complex to implement. Although filtering leaves some residual oscillation and larger uncertainties in the vicinity of the band edges, around 30 GHz and 50 GHz, this does not compromise the overall accuracy of the results

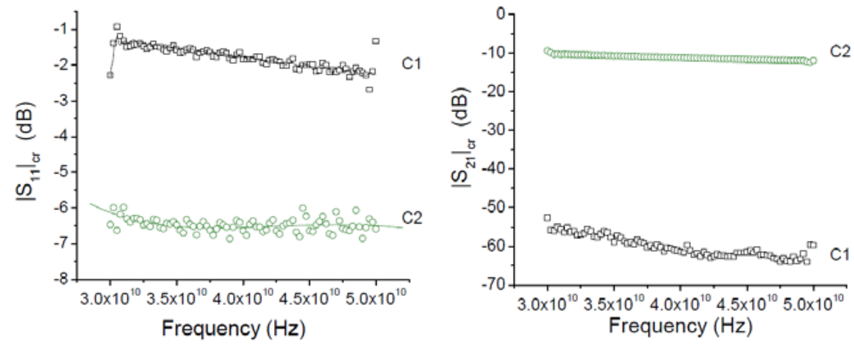


**Figure 2: Magnitude of corrected free-space scattering parameters $|S_{11}|_{cr}$ and $|S_{21}|_{cr}$ for composite materials C1 (squares) and C2 (circles) in the Q-band frequency range of 30 GHz to 50 GHz.**

[7]. In the case of composite C1 the magnitude of $S_{11\text{-}cr}$, which quantifies the reflected microwave power, is quite large, in the range of –1.5 dB at 40 GHz (> 0.8 on the linear scale).

The magnitude of the corresponding scattering parameter $S_{21\text{-}cr}$, which quantifies the microwave power transmitted through the material, is significantly smaller, about –60 dB. Such a response is characteristic of highly conducting materials, which reflect back most of the incident microwave radiation with phase angle (not shown) of about$\pi$. In comparison, composite C2 is much less reflecting, and transmits considerably more microwave power than C1. At 40 GHz, $|S_{11}|_{\text{-}cr}$ for C2 is about –9 dB and $|S_{21}|_{\text{-}cr}$ is about –10 dB. The microwave scattering parameters are useful in extracting the physical properties of the materials, such as their absorption and reflection coefficients, conductivity or microwave shielding efficiency (Fig.3). The microwave characteristics of the specimen material are represented by the complex impedance $\boldsymbol{Z}_s$, reflection coefficient $\boldsymbol{\Gamma}$, transmission coefficient $\boldsymbol{T}$ and complex propagation constant $\boldsymbol{\gamma}$. The relation between the measured scattering parameters $\boldsymbol{S}_{11}$, $\boldsymbol{S}_{21}$, and $\boldsymbol{Z}_s$, $\boldsymbol{\Gamma}$ and $\boldsymbol{T}$ are given by the following equations [9 - 11]:

$$\boldsymbol{\Gamma} = \boldsymbol{b} - \sqrt{\boldsymbol{b}^2 - 1},\ \boldsymbol{b} = \frac{\boldsymbol{S}_{11}^2 - \boldsymbol{S}_{21}^2 + 1}{\boldsymbol{S}_{11}^2},\ \ Z_s = \frac{1+\boldsymbol{\Gamma}}{1-\boldsymbol{\Gamma}}\ \text{ and }\ \boldsymbol{T} = \frac{\boldsymbol{S}_{11}^2 + \boldsymbol{S}_{21}^2 - \boldsymbol{\Gamma}}{1-(\boldsymbol{S}_{11}+\boldsymbol{S}_{21})\boldsymbol{\Gamma}}$$

The microwave absorption ($A$), and reflection ($T$), coefficients magnitude can be obtained from the power conservation formula, $A + T + R = 1$, where $T = \boldsymbol{T}\boldsymbol{T}^*$, reflectance $R = \boldsymbol{\Gamma}\boldsymbol{T}^*$, and $\boldsymbol{T}^*$ and $\boldsymbol{\Gamma}^*$ are the complex conjugate of the transmission and reflection coefficient respectively. Conductivity $\sigma$ is obtained from the complex impedance $\boldsymbol{Z}_s$,

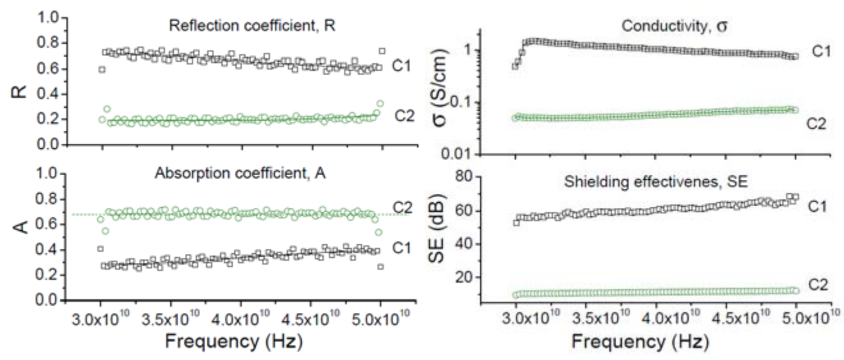


**Figure 3:Microwave reflection and absorption coefficients, conductivity and shielding effectiveness for composites C1 (squares) and C2 (circles) in the Q-band frequency range of 30 GHz to 50 GHz.**

and propagation constant $\boldsymbol{\gamma}$, [11] and the shielding effectiveness, SE, is calculated as a power loss from the reflection and absorption combined [12], SE= -20 log (1-(R+A)) (dB).

These results are shown in Figure 3. As already inferred from the scattering parameters, the C1 composite shows predominantly metallic reflectivity. As shown in Figure 3, at 40 GHz the composite C1 reflects about 66% (R=0.661) of incident microwave radiation due to its conductivity $\sigma$, which is about 1 S/cm. The conductivity of C1 decreases somewhat with frequency. This is probably due to scatter from inner structural objects that are misaligned with respect to the wave propagation direction. What is not immediately apparent from the scattering parameters shown in Fig. 2 is that C1 also absorbs about 34% (A=0.338) of incident radiation due to resistive losses. Its shielding effectiveness (SE), calculated as power loss due to the combined losses from reflection and absorption, is relatively large, SE ≈ 60 dB at 40 GHz. Considering that C1 is only 1 mm thick, such a large SE value can be achieved if the microwave skin penetration depth $\delta_e$ is smaller than the propagation length, $\delta_e = (\pi f \mu\sigma)^{-1/2} < d$, and the reflection loss is large. Table 1 lists thickness, conductivity, skin depth and shielding effectiveness for composites C1 and C2 at frequency ($f$) of 40 GHz.

Table1: Thickness (d) Conductivity (σ), Skin Penetration Depth ($\delta_e$) and Shielding Effectiveness (SE) for composites C1 and C2

| **Composite** | **d (mm)** | **σ (S/cm)** | **$\delta_e$ (μm)** | **SE (dB)** |
|---|---|---|---|---|
| C1 | 0.95 | 1.02 | 256 | 60.3 |
| C2 | 1.95 | 0.056 | 1015 | 11.2 |

The combined uncertainty of the listed measurement results is within 5%.

The skin depth of composite C1, $\delta_e$ = 256 μm is about one fourth of the thickness (t), which makes the transmitted power negligibly small. In comparison, conductivity of C2 is only 0.056 S/cm, which increases $\delta_e$ to about 1 mm. The material reflects 18% of the incident power and absorbs 65 % (Fig. 3), making SE ≈ 11.2 dB.

## SUMMARY

We presented a new free space calibration technique for non-contact measurement of electromagnetic properties of nano-carbon composites. Compared to previous calibration methods, this technique is simple to use and can be applied in real time, in a variety of testing conditions. While other methods require multiple reference values and/or movement of antennas, this technique employs only two reference measurements. The first measurement is from a known conductor, such as aluminum metal plate. The second is from an air slab with geometrical propagation length equal to that of the specimen being tested. The reconstructed conductivity and permittivity agree favorably with the values obtained using the previously reported calibration techniques. The measurement results are illustrated on nano-carbon epoxy composites with inter-laminar multi-walled carbon-nanotube structures that can be either thicker or thinner than the skin penetration depth. Depending on the arrangement of the carbon nanotube networks structures, the electromagnetic properties of these laminates can be tailored to obtain specific microwave absorbing and reflecting characteristics.

## REFERENCES


1. M. De Volder, S. Tawfick, R. Baughman, and A. Hart, *Science*, vol. 339, pp. 535-539, 2013.
2. P. Maa, N. Siddiqui, G. Marom, J. Kim, *Composites: Part A*, vol. 41, pp. 1345–1367, 2010.
3. Sara Black Composite World, May 2015. http://www.compositesworld.com/articles/nanotechnology-into-the-realm-of-real
4. D. K Ghodgaonkar, N. A. Ali, L. Giubbolini, *15th World Conference on Nondestructive Testing,* 15-21 October 2000, Roma, Italy.
5. P. Bartley, Jr. and S. Begley, *Proceedings of the IEEE Instrumentation and Measurement Technology Conference,* pp. 372-375, 2005.
6. C. Orlob, T. Reinecke, E. Denicke, B. Geck, and I. Rolfes, *IEEE Transactions on Instrumentation and Measurement,* vol. 62, no. 7, 2013.
7. A. Hassan, J. Obrzut, and E. Garboczi, *Proceedings of the Automatic RF Techniques Group 84th Microwave Measurement Conference*, Boulder, CO, Dec. 2-5, 2014. http://ieeexplore.ieee.org/xpl/articleDetails.jsp?arnumber=7013413.
8. A. Hassan and E. Garboczi, *IEEE Trans. on Antennas and Propag*., vol. 62, no. 10, pp. 5230-5241, 2014.
9. A.M. Nicolson, *IEEE Trans. Instr. Meas.*, vol 19, pp. 377–382 (1979)
10. W.R. Eisenstadt, Y. Eo, *IEEE Trans. Compo., Hybr. Manufact. Tech.*, vol 15, pp. 483–490 (1992).
11. J. Obrzut, *Measurement J.*, vol. 46 , 2963-2970 (2013).
12. http://www.learnemc.com/tutorials/Shielding01/Shielding_Theory.html.